Journal of Alloys and Compounds 652 (2015) 444–449

Contents lists available at ScienceDirect

Journal of Alloys and Compounds

journal homepage: http://www.elsevier.com/locate/jalcom

Dielectric properties of nanocomposite $(Cu)_x(SiO_2)_{(100-x)}$ produced by ion-beam sputtering

T.N. Koltunowicz [a, *], P. Zukowski [a], K. Czarnacka [a], V. Bondariev [b], O. Boiko [b], I.A. Svito [c], A.K. Fedotov [c]

[a] Department of Electrical Devices and High Voltage Technology, Lublin University of Technology, 20-618 Lublin, Poland
[b] Sumy State University, 40007 Sumy, Ukraine
[c] Belarusian State University, 220030 Minsk, Belarus

ARTICLE INFO

Article history:
Received 4 August 2015
Received in revised form
27 August 2015
Accepted 28 August 2015
Available online 2 September 2015

Keywords:
AC measurement
Electronic transport
Nanocomposites metal-dielectric

ABSTRACT

It has been established that in the nanocomposite $Cu_x(SiO_2)_{(100-x)}$ with the metallic phase content $x = 27.27$ at.% the following phenomena occur: hopping conductivity, additional polarity and coilless-like inductance. Coilless-like inductance phenomenon consists in the occurrence of positive values of phase shift in the high frequency area. Activation energy of the dielectric relaxation time for copper nanoparticles of unoxidized surface is of approx. 0.0003 eV, whereas surface oxidation causes a potential barrier occurrence and activation energy increase up to approx. 0.3360 eV. Comparative analysis of results obtained for the $Cu_x(SiO_2)_{(100-x)}$ material and the measurements results obtained for the nanocomposites $(FeCoZr)_x(Al_2O_3)_{(100-x)}$, $(FeCoZr)_x(CaF_2)_{(100-x)}$ and $(FeCoZr)_x(PZT)_{(100-x)}$, which containing nanoparticles of ferromagnetic alloy, has been performed. It has shown that the type of magnetic properties of metallic phase, which is ferromagnetic ones for FeCoZr and diamagnetic ones for Cu, does not affect capacitive and inductive phenomena of the nanocomposites. The phenomena are related only to the nanogranular structure of the materials and the hopping mechanism of the charge transport between the metallic phase nanoparticles.

1. Introduction

Nano-layers and nanocomposites draw considerable scientific attention because they exhibit properties that do not characterize materials of micro- or macro-metric structure [1]. Various methods for their production have been developed such as ion sputtering [2–4], plasma techniques [5,6] and cathodic arc deposition [7], as well as chemical technologies such as the sol–gel method [8,9]. These methods make possible to produce the granular structure [10] or nano-drops of water in oil-impregnated cellulose [11]. Such a variety of methods opens up a wide range of opportunities for investigations into electrical properties at direct [12] and alternating [13] current, as well as the mechanical, structural [14,15] and magnetic characteristics [16].

As a rule, a change in the structure size scale positively affects properties of composite nanostructures. For example, films of Zn–Ni–SiO_2 exhibit increased micro-hardness and Young's modulus [17] and other materials are characterized by superhardness and increased adhesive strength [18–21], as well as by enhanced anti-corrosion properties [22,23]. Many of the mentioned properties are conditioned by the impact of quantum-dimensional effects in a material [24]. In the case of granular nanocomposites, it is the phenomenon of electron tunneling between potential wells that are formed by metallic nanoparticles embedded in a matrix of oxides, fluorides or lead titanate salts [25–27]. Another example of the mentioned effects is a shift of spectra peaks into the area of higher quantum energy far beyond the band gap width for nanoporous silicon [28].

The hitherto performed investigations into electrical properties of metal-dielectric nanocomposites at alternating current have shown that current conduction within a certain frequency range is realized by hopping exchange of electrons [27,29,30]. The hopping exchange occurs between potential wells that are formed by metallic-phase nanograins embedded in a dielectric matrix of very high resistivity. In the $Cu_x(SiO_2)_{(100-x)}$ nanocomposites, which have been tested in this project, electrons tunnel between potential wells that are formed by nanograins of diamagnetic copper

* Corresponding author.
E-mail address: t.koltunowicz@pollub.pl (T.N. Koltunowicz).

http://dx.doi.org/10.1016/j.jallcom.2015.08.240
0925-8388/

randomly distributed in a matrix of silicon dioxide [31]. Among the phenomena that are conditioned by electron tunneling in granular metal-dielectric nanocomposites is a phenomenon of coilless-like inductance. It consists in the occurrence of positive values of the phase difference in the frequency dependences [32] as well as in the formation of dipoles [33], whose orientation is ordered by an external electric field, which leads to an increase of the dielectric permittivity relative to the matrix material [13].

The objective of the discussed research project has been to experimentally examine polarization and conductivity phenomena that occur at alternating current in nanocomposites $Cu_x(SiO_2)_{(100-x)}$ produced by ion-beam sputtering using argon ions, depending on the alternating current frequency and the measuring temperature as well as to analyze the mechanism of the occurrence of elevated dielectric permittivity in the nanocomposites.

2. Experimental results and their analysis

2.1. Experimental

For the testing purposes, samples of the nanocomposite $Cu_x(SiO_2)_{(100-x)}$ with the metallic phase content ranging from 9 to 73 at.% have been used. The samples have been produced by ion-beam sputtering of a target composed of copper and strips of the SiO_2 dielectric. A detailed description of producing the metal-dielectric nanocomposites can be found in Refs. [2,10]. The sputtering has been performed with a beam of argon ions of the pressure of $P_{Ar} = 4 \times 10^{-3}$ Pa.

Chemical composition has been determined with the application of the scanning electron microscopy (SEM) using a LEO 1455VP microscope as well as of the X-ray microanalysis (EDX). The error at determining the content of individual elements has been lower than ±1%.

The paper presents measurement results obtained for a newly produced sample of the $Cu_x(SiO_2)_{(100-x)}$ nanocomposite with the metallic phase content $x = 27.27$ at.% – i.e. below the percolation threshold.

Measurements of frequency and temperature dependences of the phase shift θ, loss tangent tan δ, capacitance C_p and conductivity σ have been performed at a laboratory setup for AC-based testing of the nanocomposite electrical properties that has been described in Ref. [34]. The obtained samples have been tested at alternating current of the frequency ranging from 50 Hz to 5 MHz, and measuring temperatures of $T_p = 77$ K – 373 K at the temperature change step of 5°K.

2.2. Analysis of the measurement results

Fig. 1 shows the phase shift vs. frequency dependence for a freshly produced sample of the $Cu_x(SiO_2)_{(100-x)}$ nanocomposite of the metallic phase content $x = 27.27$ at.% for selected measuring temperatures ranging from LNT to 273 K. As can be seen, in the low frequency area the phase shift values are negative ($\theta < 0°$). The increasing frequency makes the phase shift value gradually approach zero. At a certain frequency f_R, that depends on the measuring temperature, the phase shift value reaches zero ($\theta = 0°$). Further frequency increase leads to the phase shift transition to the area of positive values ($\theta > 0°$). This phase shift vs. frequency characteristic resembles a relation that is characteristic for a conventional *RLC* series circuit composed of discrete elements: a resistor *R*, a capacitor *C* and a coil of the inductance *L*. In that circuit, a phenomenon of voltage resonance occurs at the frequency f_R [25,32]. This means that at frequency values that exceed the resonance frequency ($f > f_R$), in the tested nanocomposite the AC induction-type conductivity occurs. A thin nanocomposite film has been used for the testing. Such a film does not include any windings that are characteristic for a coil and the coilless-like inductance phenomenon is produced by the mechanism of hopping current conduction [35]. The occurrence of voltage resonance is accompanied by the below discussed phenomena. First, at frequencies approaching f_R voltage compensation occurs at the capacitance U_C (the phase shift is $\theta_C = -90°$ relative to the excitation voltage) and at the inductance U_L (the phase shift angle is $\theta_L = +90°$ relative to the excitation voltage). Thus, the imaginary part of voltage decreases and at the frequency f_R reaches down to zero. This is illustrated in Fig. 2, where the tan δ values are shown. As can be seen in this figure, at frequencies approaching f_R the tan $\delta > 10$, meaning that the values of imaginary voltage component are negligible. In *RLC* circuits a real voltage component U_R and its two imaginary parts– capacitive one (U_C) and inductive one (U_L) occur.

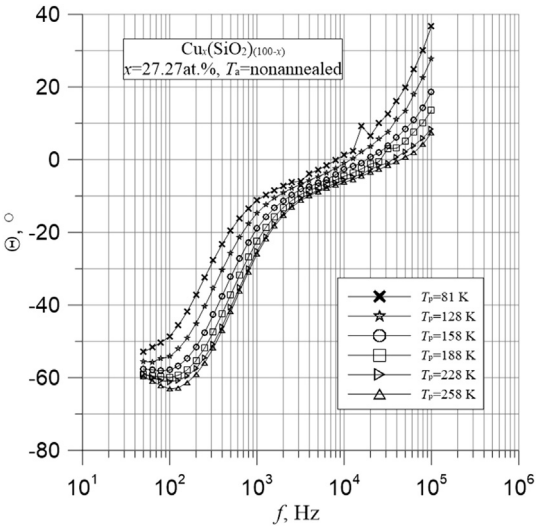

Fig. 1. Phase shift vs. frequency dependence obtained for a freshly produced sample of the $Cu_x(SiO_2)_{(100-x)}$ nanocomposite of the metallic phase content $x = 27.27$ at.% at selected measuring temperatures T_p: *1*–81 K, *2*–128 K, *3*–158 K, *4*–188 K, *5*–228 K, *6*–258 K.

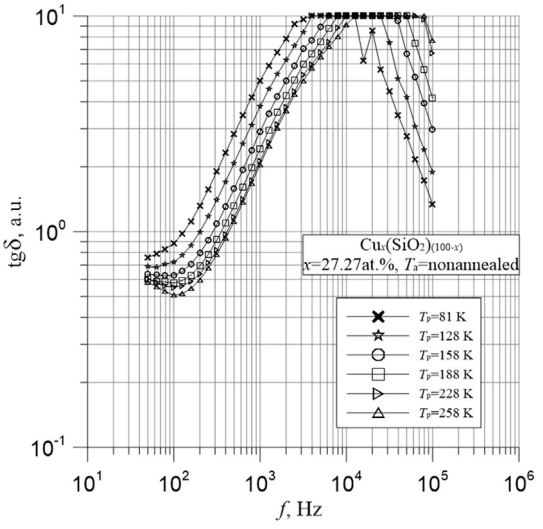

Fig. 2. Loss tangent *tg δ* vs. frequency dependence obtained for a freshly produced sample of the $Cu_x(SiO_2)_{(100-x)}$ nanocomposite of the metallic phase content $x = 27.27$ at.% at selected measuring temperatures T_p: *1*–81 K, *2*–128 K, *3*–158 K, *4*–188 K, *5*–228 K, *6*–258 K.

Impedance meters (*RLC* meters) clearly determine the real voltage component and the circuit resistance R that is related to it, while measurements of the capacitive component U_C are affected by the inductive component U_L that occurs simultaneously to it. This means that an impedance meter can measure a value of capacitance of a *RLC* series circuit only at low measuring frequencies i.e. far away from the resonance frequency ($f << f_R$), where the phase shift is $\theta \approx -90°$.

Fig. 3 presents selected capacitance vs. frequency dependences obtained for a newly produced sample of the nanocomposite $Cu_x(SiO_2)_{(100-x)}$ with the metallic phase content $x = 27.27$ at.%. As can be seen in this figure, in the low frequency area ($f < 10^2$ Hz), the value of capacitance is almost constant. Further frequency increase makes the capacitance value rapidly decrease till it reaches a sharp local minimum, whose location depends on the measuring temperature. Comparative analysis of plots of the phase shift (Fig. 1) and the capacitance (Fig. 3) indicates that the local minimum in the $C(f)$ characteristic occurs at the same frequency as the phase shift zero-crossing that is at the resonance frequency f_R, where the compensation of the imaginary voltage components i.e. the capacitive voltage U_C and the inductive voltage U_L occurs. At the further frequency increase, the inductive component grows larger than the capacitive one and the phase shift enters the area of positive values.

Fig. 4 presents selected conductivity vs. frequency dependences obtained for a newly produced sample of the nanocomposite $Cu_x(SiO_2)_{(100-x)}$ with the metallic phase content $x = 27.27$ at.%. As can be seen in this figure, the frequency increase makes the conductivity value first grow and then almost stabilize. A model of hopping charge exchange at direct and alternating current proposed in Refs. [13,33] and developed in Refs. [34,36] has been applied to the analysis of frequency dependences of the phase shift (Fig. 1), loss tangent (Fig. 2), capacitance (Fig. 3) and conductivity (Fig. 4).

According to the model, hopping exchange of charges occurs between metallic-phase nanoparticles embedded in a dielectric matrix. The exchange can be realized by tunneling. A hop from one neutral particle to another causes the dipole formation (additional polarization of the material). As the dipole lifetime τ elapses, another electron hop occurs in the opposite direction to the electric field (direct current). Such hops occur at the probability p that is rather low. When the time τ elapses, the remaining electrons (1-p) under the influence of the dipole local electric field return to the particles, wherefrom they started their hopping. This produces a passage of high-frequency current and makes the dipoles vanish. It follows from the model, that in the low frequency area an additional thermally-activated polarization occurs – the capacitance grows along with the increasing temperature. Within the mentioned frequency range, the conductivity is hardly frequency dependent. In order to determine the dielectric relaxation time value, dependences of the imaginary permittivity component ε'' have been determined based on the below given formula:

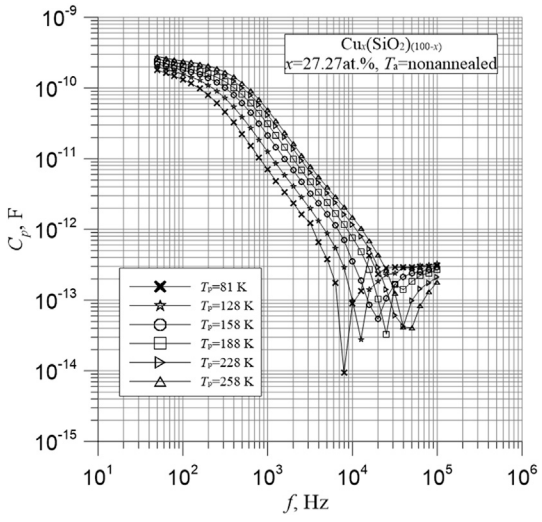

Fig. 3. Capacitance vs. frequency dependence obtained for a freshly produced sample of the $Cu_x(SiO_2)_{(100-x)}$ nanocomposite of the metallic phase content $x = 27.27$ at.% at selected measuring temperatures T_p: *1*–81 K, *2*–128 K, *3*–158 K, *4*–188 K, *5*–228 K, *6*–258 K.

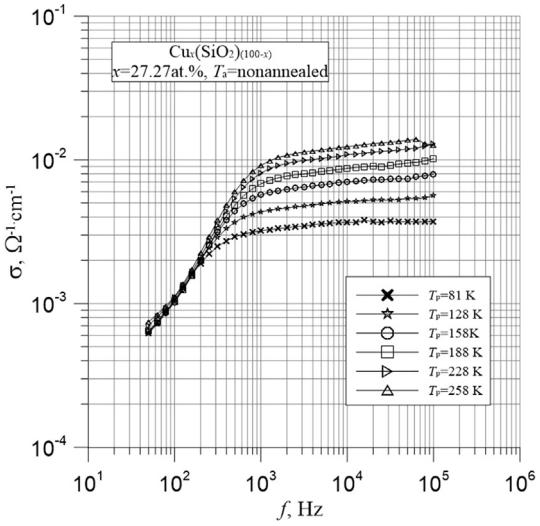

Fig. 4. Conductivity vs. frequency dependence obtained for a freshly produced sample of the $Cu_x(SiO_2)_{(100-x)}$ nanocomposite sample of the metallic phase content $x = 27.27$ at.% at selected measuring temperatures T_p: *1*–81 K, *2*–128 K, *3*–158 K, *4*–188 K, *5*–228 K, *6*–258 K.

$$\varepsilon'' = \frac{\sigma}{\varepsilon_0 \cdot \omega} \tag{1}$$

where ε'' – imaginary part of the permittivity; σ – conductivity; ε_0 – free space permittivity; $\omega = 2\pi f$ – angular frequency.

As is well known [37], the imaginary permittivity component reaches its maximum value at the angular frequency of:

$$\omega_{max} = \frac{1}{\tau} \tag{2}$$

By determining the location of that maximum in the characteristic $\varepsilon''(\omega)$ with the formula (2), it is possible to determine values of the dipole lifetime τ (dielectric relaxation time). Fig. 5 shows the imaginary permittivity vs. angular frequency characteristics for selected measuring temperatures. Based on those plots, locations of the maxima have been determined for individual measuring temperatures, and on that basis – the values of τ.

The dielectric relaxation time τ can be described with the following formula [38,39]:

$$\tau(T) = \tau_0 \cdot \exp\left(\frac{\Delta E_\tau}{k \cdot T}\right) \tag{3}$$

Fig. 6 presents an Arrhenius plot for the dipole lifetime τ. As can be seen in the plot, in the low temperature area a weak temperature dependence of the time τ occurs, which corresponds to the low value of the activation energy $\Delta E_{1\tau} \approx 0.0003$ eV.

Electrons tunneling through the dielectric layer from one

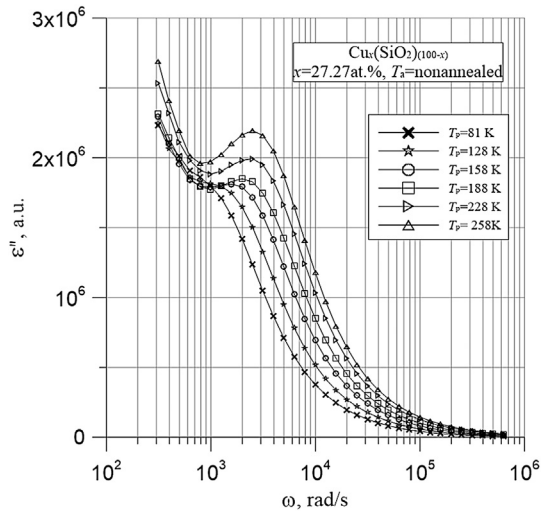

Fig. 5. Imaginary part of the permittivity vs. angular frequency dependence obtained for a freshly produced sample of the $Cu_x(SiO_2)_{(100-x)}$ nanocomposite of the metallic phase content $x = 27.27$ at.%. Measuring temperatures T_p: *1*–81 K, *2*–128 K, *3*–158 K, *4*–188 K, *5*–228 K, *6*–258 K.

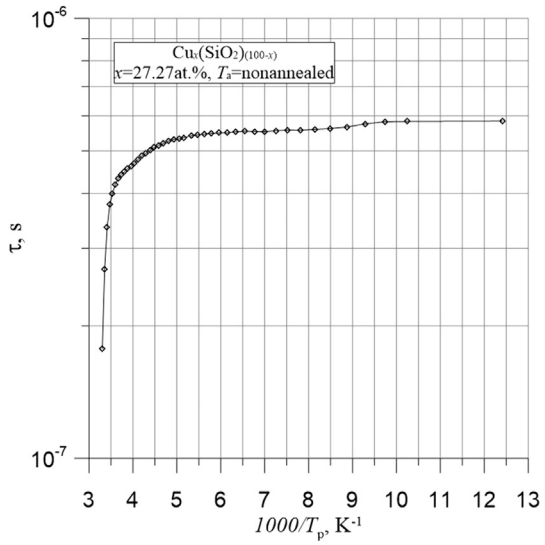

Fig. 6. Dipole lifetime τ vs. inverse temperature for a freshly produced sample of the $Cu_x(SiO_2)_{(100-x)}$ nanocomposite of the metallic phase content $x = 27.27$ at.%.

metallic phase nanoparticle to the second take place from the uppermost level manned by an electron at the lowest unoccupied level. These levels are close to the Fermi level. The nanoparticles of the metallic phase have a shape close to the spherical and their average dimensions amounts approx. 6 nm. Such a molecule contains about 10 000 atoms and the same number of levels is in the conduction band. Because the width of the conduction band in metals is a few eV, the distance between levels should be a few tenthousandths of electron-volts, which is in accordance with activation energy value $\Delta E_{1\tau} \approx 0.0003$ eV obtained from the Arrhenius graph.

In the area of high temperatures, the activation energy multiply increases up to the value of $\Delta E_{2\tau} \approx 0.336$ eV. This is related to the fact that there are two types of nanoparticles in the tested nanocomposite. The first one includes particles of the metallic phase. Due to the fact that in the metal conduction band there are both electrons (below the Fermi level) and empty states (above that level), the tunneling between such nanoparticles is realized at low activation energy. Particles of the other are covered by an oxide layer that forms a high potential barrier. As a hopping electron has to overcome the potential barrier, the hopping from unoxidized particles onto the oxidized ones as well as from the oxidized ones onto the oxidized or unoxidized ones requires high activation energy.

Fig. 7 shows an Arrhenius plot for low frequency capacitance measured at the frequency of 100 Hz. As in the Arrhenius plot for τ (Fig. 6), in the plot for C (Fig. 7) two increase stages can be observed. The first one of low activation energy of $\Delta E_{1C} \approx 0.007$ eV in the low temperature area and the other one of higher activation energy of $\Delta E_{2C} \approx 0.418$ eV and in the area of high temperatures.

Our earlier publications have presented results of investigations into nanocomposites that contain metallic phase nanoparticles of in the form of ferromagnetic alloy $Fe_{45}Co_{45}Zr_{10}$, embedded in dielectric matrices of Al_2O_3 [27], CaF_2 [26,29,30,32,36] and of ferroelectric PZT [32,35]. In those nanocomposites like in the case of the presently discussed $Cu_x(SiO_2)_{(100-x)}$ material, in the low frequency region negative values of the phase shift occur. Frequency increase leads to the occurrence of the voltage resonance phenomenon followed by the phase shift transition to the area of positive values i.e. by the occurrence of the coilless-like inductance phenomenon. Reviewers of the publications concerning nanocomposites that contain $Fe_{45}Co_{45}Zr_{10}$ nanoparticles have indicated possible impact of the nanoparticle ferromagnetism on the occurrence of the coilless-like inductance in those materials. Testing of the $Cu_x(SiO_2)_{(100-x)}$ nanocomposite has shown that the mentioned phenomenon occurs also in materials that do not contain any ferromagnetic alloy. This means that the presently discussed phenomena that occur in the $Cu_x(SiO_2)_{(100-x)}$ nanocomposite that is the capacitance, conductivity and inductance are related to the hopping exchange of charges between nanoparticles of the metallic phase.

3. Conclusions

The paper presents results of investigations into frequency and temperature dependences of the phase shift, loss tangent,

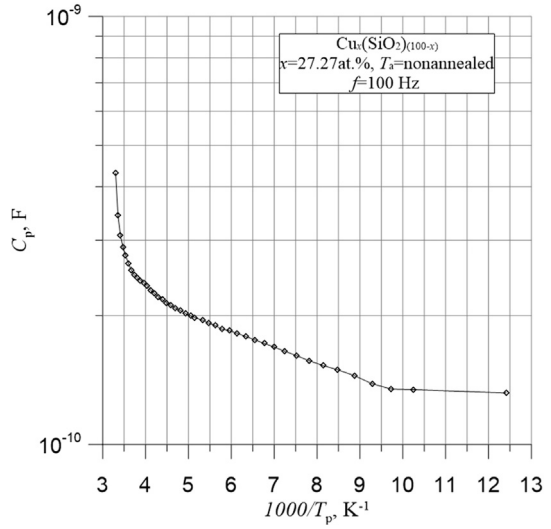

Fig. 7. Low-frequency capacitance (100 Hz) vs. inverse temperature for a freshly produced sample of the $Cu_x(SiO_2)_{(100-x)}$ nanocomposite of the metallic phase content $x = 27.27$ at.%.

capacitance and conductivity of the $Cu_x(SiO_2)_{(100-x)}$ nanocomposite with the metallic phase content $x = 27.27$ at.%. It has been found that in that nanocomposite the following phenomena occur: hopping conductivity, additional polarity relative to the matrix and coilless-like inductance that consists in the occurrence of positive phase shift values in the high frequency area. Temperature dependence of the dielectric relaxation time has been determined. It indicates that some of the copper nanoparticles that occur in the material are covered by a layer of copper oxides that forms a potential barrier and increases the dielectric relaxation time activation energy to the value of approx. 0.336 eV in the area of elevated temperatures. Relaxation time activation energy for nanoparticles without the oxide layer is much lower. Its value is of approx. 0.0003 eV. Comparative analysis of results obtained for the $Cu_x(SiO_2)_{(100-x)}$ material and for the nanocomposites $(FeCoZr)_x(Al_2O_3)_{(100-x)}$, $(FeCoZr)_x(CaF_2)_{(100-x)}$ and $(FeCoZr)_x(PZT)_{(100-x)}$, that contain nanoparticles of ferromagnetic alloy has been performed. The analysis has shown that capacitive and inductive properties that characterize all the examined materials are related only to the nanogranular structure of those materials and to the hopping mechanism of the charge transport between nanoparticles of the metallic phase. The type of magnetic properties of the metallic phase – ferromagnetic for FeCoZr and diamagnetic for Cu does not affect the capacitive and inductive phenomena of those nanocomposites.

Acknowledgments

This research was funded from the statute tasks of the Lublin University of Technology, at the Faculty of Electrical Engineering and Computer Science, S-28/E/2015, entitled 'Preparation of nanolayers and nanocomposites metal or semiconductor in the dielectric matrix and the study of their electrical and magnetic properties' and the statute grant for PhD students.

References

[1] A.D. Pogrebnjak, V.M. Beresnev, Nanocoatings Nanosystems Nanotechnologies, Bentham Science, Oak Park, IL, 2012.
[2] I.V. Zolotukhin, YuE. Kalinin, A.T. Ponomarenko, V.G. Shevchenko, A.V. Sitnikov, O.V. Stognei, O. Figovsky, Metal-dielectric nanocomposites with amorphous structure, J. Nanostructured Polym. Nanocomposites 2 (2006) 23–34.
[3] F.F. Komarov, A.V. Leontyev, V.V. Grigoryev, M.A. Kamishan, Ion implantation for local change of the optical constants of polymer films, Nucl. Instrum. Methods Phys. Res. B 191 (2002) 728–732.
[4] R.F. Haglund Jr., Ion implantation as a tool in the synthesis of practical third-order nonlinear optical materials, Mater. Sci. Eng. A 253 (1998) 275–283.
[5] H. Sari, V.M. Astashynski, E.A. Kostyukevich, A.M. Kuzmitski, V.V. Uglov, N.N. Cherenda, YuA. Petukhou, Austenitic steel surface alloyed with zirconium using compression plasma flow, High. Temp. Mater. Process. 16 (n.4) (2012) 297–313.
[6] A.H. Sari, V.M. Astashynski, S.I. Ananin, E.A. Kostyukevich, A.M. Kuzmitski, V.V. Uglov, N.N. Cherenda, Alloying of carbon steel surface by tantalum using compression plasma flow, High. Temp. Mater. Process. 17 (n.1) (2013) 47–73.
[7] A.D. Pogrebnjak, Structure and properties of nanostructured (Ti-Hf-Zr-V-Nb)N coatings, J. Nanomater. (2013). Article ID: 780125 (12 pages).
[8] R.S.R. Kalidindi, R. Subasri, 5 – Sol-gel nanocomposite hard coatings, Anti-Abrasive Nanocoatings Curr. Future Appl. (2015) 105–136, http://dx.doi.org/10.1016/B978-0-85709-211-3.00005-4.
[9] L.P. Singh, S.K. Bhattacharyya, R. Kumar, G. Mishra, U. Sharma, G. Singh, S. Ahalawat, Sol-Gel processing of silica nanoparticles and their applications, Adv. Colloid Interface Sci. 214 (2014) 17–37.
[10] YuE. Kalinin, A.T. Ponomarenko, A.V. Sitnikov, O.V. Stogney, Granular metal-insulator nanocomposites with amorphous structure, Phys. Chem. Mater. Treat. 5 (2001) 14–20.
[11] P. Żukowski, T.N. Kołtunowicz, K. Kierczyński, J. Subocz, M. Szrot, M. Gutten, Assessment of water content in an impregnated pressboardbased on DC conductivity measurements. Theoretical assumptions, IEEE Trans. Dielectr. Electr. Insulation 21 n.3 (2014) 1268–1275.
[12] P. Zukowski, T.N. Kołtunowicz, K. Kierczynski, J. Subocz, M. Szrot, Formation of water nanodrops in cellulose impregnated with insulating oil, Cellulose 22 (2015) 861–866.
[13] P.W. Zukowski, A. Rodzik, Y.A. Shostak, Dielectric constant and ac conductivity of semi-insulating $Cd_{1-x}Mn_xTe$ semiconductors, Semiconductors 31 (n.6) (1997) 610–614.
[14] A.D. Pogrebnjak, A.G. Ponomarev, A.P. Shpak, YuA. Kunitskii, Application of micro- and nanoprobes to the analysis of small-sized 3D materials, nano-systems, and nanoobjects, Physics-Uspekhi 55 n.3 (2012) 270–300.
[15] N. Prokopchuk, V. Luhin, K. Vishnevskii, Z. Shashok, P. Zukowski, J. Plowucha, SEM investigation of chitosan nanofibers produced by nanospider technology, High. Temp. Mater. Process. 17 (n.2–3) (2013) 195–203.
[16] J. Fedotova, A. Saad, D. Ivanou, Y. Ivanova, A. Fedotov, A. Mazanik, I. Svito, E. Streltsov, T.N. Koltunowicz, S. Tyutyunnikov, Gigantic magnetoresistive effect in n-Si/SiO_2/Ni nanostructures fabricated by the template-assisted electrochemical deposition, Przeglad Elektrotechniczny 88 (n.7a) (2012) 305–308.
[17] N.I. Poliak, V.M. Anishchik, N.G. Valko, C. Karwat, C. Kozak, M. Opielak, Mechanical properties of Zn-Ni-SiO_2 coating deposited under X-ray irradiation, Acta Phys. Pol. A 125 (n.6) (2014) 1415–1417.
[18] A.D. Pogrebnjak, V.M. Beresnev, A.A. Demianenko, V.S. Baidak, F.F. Komarov, M.V. Kaverin, N.A. Makhmudov, D. Kolesnikov, Adhesive strength, superhardness, and the phase and elemental compositions of nanostructured coatings based on Ti-Hf-Si-N, Phys. Solid State 54 (n.9) (2012) 1882–1890.
[19] O.V. Sobol, A.D. Pogrebnyak, V.M. Beresnev, Effect of the preparation conditions on the phase composition, structure, and mechanical characteristics of vacuum-Arc Zr-Ti-Si-N coatings, Phys. Metals Metallogr. 112 (n.2) (2011) 188–195.
[20] A.D. Pogrebnjak, G. Abadias, O.V. Bondar, B.O. Postolnyi, M.O. Lisovenko, O.V. Kyrychenko, A.A. Andreev, V.M. Beresnev, D.A. Kolesnikov, M. Opielak, Structure and properties of multilayer nanostructured coatings TiN/MoN depending on deposition conditions, Acta Phys. Pol. A 125 (n.6) (2014) 1280–1283.
[21] F.F. Komarov, S.V. Konstantinov, A.D. Pogresnjak, V.V. Pilko, C. Kozak, M. Opielak, formation and characterization of nanostructured composite coatings based on the TiN phase, Acta Phys. Pol. A 125 (n.6) (2014) 1292–1295.
[22] N.D. Nghia, N.T. Tung, Study on synthesis and anticorrosion properties of polymer nanocomposites based on super paramagnetic Fe_2O_3 center dot NiO nanoparticle and polyaniline, Synth. Met. 159 (n.9–10) (2009) 831–834.
[23] B. Ramezanzadeh, M.M. Attar, M. Farzam, A study on the anticorrosion performance of the epoxy-polyamide nanocomposites containing ZnO nanoparticles, Progres Org. Coatings 72 (n.3) (2011) 410–422.
[24] Y. Imry, Introduction to Mesoscopic Physics, University Press, Oxford, 2002.
[25] T.N. Kołtunowicz, J.A. Fedotova, P. Zhukowski, A. Saad, A. Fedotov, J.V. Kasiuk, A.V. Larkin, Negative capacitance in (FeCoZr)-(PZT) nanocomposite films, J. Phys. D Appl. Phys. 46 (n.12) (2013) 125304 (10 pages).
[26] T.N. Koltunowicz, P. Zhukowski, V. Bondariev, A. Saad, J.A. Fedotova, A.K. Fedotov, M. Milosavljevic, J.V. Kasiuk, Enhancement of negative capacitance effect in $(FeCoZr)_x(CaF_2)_{(100-x)}$ nanocomposite films deposited by ion beam sputtering in argon and oxygen atmosphere, J. Alloys Compd. 615 (Suppl. 1) (2014) S361–S365.
[27] I. Svito, J.A. Fedotova, M. Milosavljević, P. Zhukowski, T.N. Koltunowicz, A. Saad, K. Kierczynski, A.K. Fedotov, Influence of sputtering atmosphere on hopping conductance in granular nanocomposite $(FeCoZr)_x(Al_2O_3)_{1-x}$ films, J. Alloys Compd. 615 (Suppl. 1) (2014) S344–S347.
[28] J. Zuk, R. Kuduk, M. Kulik, J. Liskiewicz, D. Maczka, P.V. Zhukovski, V.F. Stelmakh, V.P. Bondarenko, A.M. Dorofeev, Ionoluminescence of porous silicon, J. Luminescence 57 (n.1–6) (1993) 57–60.
[29] T.N. Kołtunowicz, P. Zhukowski, V. Bondariev, J.A. Fedotova, A.K. Fedotov, Annealing of $(CoFeZr)_x(CaF_2)_{(100-x)}$ nanocomposites produced by the ion-beam sputtering in the Ar and O_2 ambient, Acta Phys. Pol. A 123 (n.5) (2013) 932–934.
[30] T.N. Koltunowicz, P. Zukowski, M. Milosavljević, A.M. Saad, J.V. Kasiuk, J.A. Fedotova, YuE. Kalinin, A.V. Sitnikov, A.K. Fedotov, AC/DC conductance in granular nanocomposite films $(Fe_{45}Co_{45}Zr_{10})_x(CaF_2)_{100-x}$, J. Alloys Compd. 586 (Suppl. 1) (2014) S353–S356.
[31] I. Svito, A.K. Fedotov, T.N. Koltunowicz, P. Zhukowski, Y. Kalinin, A. Sitnikov, K. Czarnacka, A. Saad, Hopping of electron transport in granular $Cu_x(SiO_2)_{1-x}$ nanocomposite films deposited by ion-beam sputtering, J. Alloys Compd. 615 (Suppl. 1) (2014) S371–S374.
[32] T.N. Koltunowicz, Inductive type properties of FeCoZr-CaF_2 and FeCoZr-PZT nanocomposites, J. Mater. Sci. Mater. Electron. 26 (n.9) (2015) 6450–6457. http://link.springer.com/journal/10854/26/9/page/1.
[33] P.W. Zukowski, S.B. Kantorow, K. Kiszczak, D. Maczka, V.F. Stelmakh, A. Rodzik, E. Czarnecka-Such, Study of dielectric function of silicon irradiation with great dose of neutrons, Phys. Status Solidi A – Appl. Res. 128 (n.2) (1991) K117–K121.
[34] F.F. Komarov, P. Zhukowski, R.M. Krivosheev, E. Munoz, T.N. Koltunowicz, V.N. Rodionova, A.K. Togambaeva, Effects of surfactant and fabrication procedure on the electrical conductivity and electromagnetic shielding of single-walled carbon nanotube films, Phys. Status Solidi A – Appl. Mater. Sci. 212 (n.2) (2015) 425–432.
[35] T.N. Kołtunowicz, P. Żukowski, O. Boiko, V. Bondariev, K. Czarnacka, J.A. Fedotova, A.K. Fedotov, I.A. Svito, Impedance model of metal-dielectric nanocomposites produced by ion-beam sputtering in vacuum and its experimental verification for thin films of $(FeCoZr)_x(PZT)_{(100-x)}$, Vacuum (2015), http://dx.doi.org/10.1016/j.vacuum.2015.04.035.
[36] T.N. Kołtunowicz, P. Żukowski, V. Bondariev, J.A. Fedotova, A.K. Fedotov, The effect of annealing on the impedance of $(FeCoZr)_x(CaF_2)_{(100-x)}$ nanocomposite

films produced by the ion-beam sputtering in vacuum, Vacuum (2015), http://dx.doi.org/10.1016/j.vacuum.2015.01.030.
[37] A.K. Jonscher, Dielectric Relaxation in Solids, Chelsea Dielectrics Press, London, 1983.
[38] G.C. Psarras, E. Manolakaki, G.M. Tsangaris, Dielectric dispersion and ac conductivity in-Iron particles loaded-polymer composites, Compos. Part A Appl. Sci. Manuf. 34 (n.12) (2003) 1187–1198.
[39] M.A. Kudryashov, A.I. Mashin, A.A. Logunov, G. Chidichimo, G. De Filpo, Frequency dependence of the electrical conductivity in Ag/PAN nanocomposites, Tech. Phys. 57 (n.7) (2012) 965–970.